Food Chemistry: X 25 (2025) 102088

Contents lists available at ScienceDirect

Food Chemistry: X

journal homepage: www.sciencedirect.com/journal/food-chemistry-x

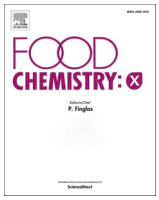

Mechanistic studies on the effect of endogenous proteins on the starch retrogradation characteristics of corn before and after postharvest ripening

Nannan Hu [a,b,c,1], Weihua Qi [b,1], Jinying Zhu [a,c], Fuyin Zhao [a,c], Lin Xiu [a,c], Mingzhu Zheng [a,c,*], Jingsheng Liu [a,c,*]

[a] College of Food Science and Engineering, Jilin Agricultural University, Changchun, Jilin 130118, China
[b] School of Life Science, Changchun Sci-Tech University, Changchun, Jilin 130600, China
[c] National Engineering Research Center for Wheat and Corn Deep Processing, Changchun, Jilin 130118, China

ARTICLE INFO

Keywords:
Starch
Retrogradation
Protein
Postharvest ripening
Interaction

ABSTRACT

The corn starch-protein complexes before postharvest ripening (JD-0) and after postharvest ripening (JD-40) were subjected to protease treatment, and the influence of protein on starch retrogradation was studied. Kinetic studies of starch retrogradation showed that protein reduced the retrogradation rate constant (k) of starch by 25.46 % (JD-0) and 7.48 % (JD-40), respectively. This was mainly reflected in the inhibition of short-range order, relative crystallinity and helix structure formation in the retrogradation process. In addition, low field strength nuclear magnetic resonance (LF-NMR) analyses also revealed that proteins inhibited starch retrogradation by isolating the precipitation of free water during retrogradation, causing the decrease in the viscoelasticity and firmness of the starch gel. Therefore, the inhibitory effect of proteins on starch retrogradation before postharvest ripening of corn-based food products was more relevant.

1. Introduction

Corn has an important economic and social value as one of the high yielding cereals globally. In 2023, global corn production reached 1.229 billion tons. Corn is a postharvest ripening crop. Newly harvested corn is stored for several days to months before consumption and processing, during which time its eating quality and processing characteristics are improved. It had been demonstrated that post-ripened corn had improved starch gel formation (Hu et al., 2023) and improved digestibility of zein (Zhao et al., 2022).

Corn-based meals exhibit a greater tendency for retrogradation when stored at low temperatures following cooking. Starch retrogradation was often considered an undesirable phenomenon due to its negative impact on the texture, viscosity, and water-binding properties of baked products. The water retention capacity of starch-rich meals was reduced due to the process of starch retrogradation, which consequently resulted in a decline in both shelf life and consumer acceptance (Zhang et al., 2014). Nevertheless, starch retrogradation might be used in certain applications, such as the manufacturing of morning cereals, steaming cereal rice, and rice flour (Wang et al., 2015). The retrogradation of starch was typically influenced by the fine structure of starch molecules, encompassing the molecular size and chain length distribution of amylose and amylopectin (Li et al., 2021; Zhang et al., 2021). Additionally, other components in starch-based foods could also affect the retrogradation properties of starch, such as water (Zhang et al., 2022) and protein content.

Protein, as the second major constituent of corn kernels, had a significant impact on starch retrogradation properties. The impact of proteins on starch retrogradation also varied depending on the kind of protein (source, amino acid sequence, structure, etc.), the type of starch (source, ratio of amylose/amylopectin, etc.), and the ratio of protein to starch. Lu et al. (2016) found that protein addition inhibited starch solubilization, and DSC and rheological characterization showed that low protein additions (5 % and 10 %) promoted amylopectin retrogradation, but high protein additions (15 %) inhibited amylopectin retrogradation. Lian et al. (2014) showed that wheat gluten fractions inhibited the retrogradation of wheat starch, whereas the albumin, globulin, and zein fractions facilitated starch retrogradation. There were still differing opinions on the impact of proteins on starch retrogradation. Several researches have shown that the presence of proteins

* Corresponding authors at: College of Food Science and Engineering, Jilin Agricultural University, Changchun, Jilin 130118, China.
E-mail addresses: Zhengmzhu@163.com (M. Zheng), liujingsheng@jlau.edu.cn (J. Liu).
[1] These authors contributed equally.

https://doi.org/10.1016/j.fochx.2024.102088
Received 1 September 2024; Received in revised form 4 December 2024; Accepted 9 December 2024
Available online 10 December 2024

inhibits starch retrogradation (Lian et al., 2013; Zhang et al., 2019). Proteins that had a greater number of hydrophilic groups or possessed a high ability to bind water might hinder the process of starch retrogradation by limiting the movement of water molecules. Additionally, these hydrophilic groups might facilitate the establishment of hydrogen bonds between starch and protein, hence inhibiting the creation of junction zones. Using low-field NMR, Zhang et al. (2019) found that adding 10 % of rice protein to rice starch would result in a reduction of the free water fraction and an increase in the proportions of bound water and semi-bound water. On the other hand, proteins were able to penetrate the starch matrix and reduce the density of the starch structure, thereby impeding the creation of hydrogen bonds between amylose molecules. The presence of reactive polyhydroxyl groups in rice protein hydrolysates might effectively inhibit the retrogradation of rice/wheat starch. This was achieved by blocking the formation of hydrogen bonds between starch molecules (Niu et al., 2017; Zhang et al., 2020). In addition, hydrophobic amino acid residues situated on the exterior surface of proteins tend to repel water from starch granules. This interaction limited both solubilization and the migration of water molecules, thereby inhibiting starch retrogradation. Kuang et al. (2022) showed that zein inhibited the starch retrogradation of amylose because the production of amylose-zein complexes occurred via hydrophobic interactions. And other studies had shown that proteins could promote retrogradation (Chen et al., 2019; Scott & Awika, 2023). Proteins with high surface hydrophobicity could promote starch retrogradation by repelling water from starch granules during protein aggregation. When hydrogen bonds were formed by aggregation between proteins, it could lead to protein precipitation and also accelerate starch retrogradation (Nicolai & Durand, 2013).

Starch and protein in natural corn kernels exist in a composite structure. Our previous studies have demonstrated the presence of hydrophobic interactions and hydrogen bonding between the two, and a tendency for this interaction to diminish after postharvest ripening (Hu et al., 2024). Under the influence of this interaction, the effect of protein in corn kernels on the retrogradation properties of starch after postharvest ripening is not yet clear. Therefore, this study examined the mechanism of endogenous proteins on starch retrogradation of corn before and after postharvest ripening. The aim is to offer reference and guidance for the suitability of corn flour processing before and after postharvest ripening and the prolongation of the shelf life of corn food products.

2. Materials and methods

2.1. Materials

The corn used in this investigation was the same as that used in our previous publication (Hu et al., 2024). Alkaline protease (S10154, 200 U/mg) was acquired from Shanghai Yuanye Biotechnology Co., Ltd. (Shanghai, China).

2.2. Preparation of samples

Corn kernels that were not ripened after harvest and were ripened after harvest were immersed in deionized water at a temperature of 4 °C for a duration of 24 h. They were then stripped of their seed coat and germ, freeze-dried, and crushed to get starch-protein complexes. The resulting complexes were designated as JD-0 and JD-40, respectively. The method of Li et al. (2023) was referenced and briefly modified. Briefly, 10 g of the complex sample was weighed and added to 80 mL of sodium carbonate buffer solution (0.02 M, pH 9.0) of alkaline protease with an enzyme activity of 200 U/mL, and the proteins were removed by continuous stirring for 8 h in a water bath at 40 °C. The suspension was then centrifuged for 10 min at 4000 rpm, and stirring and centrifugation were repeated twice. The precipitates were rinsed with distilled water until they reached a neutral pH. The obtained protein-free samples were then desiccated at 40 °C for 48 h, ground, and labeled as JD-0-DP (sample that had not undergone postharvest ripening) and JD-40-DP (sample that had postharvest ripened at 15 °C for 40 days), respectively.

The above samples (JD-0, JD-0-DP, JD-40, and JD-40-DP) were completely pasteurized by RVA and then stored at 4 °C for 1 and 21 days, respectively, to determine the rheological, gel textural characteristics and the laws of water migration of the samples with different retrogradation days. A portion of the samples with different retrogradation times were freeze-dried, ground, sieved through an 80 mesh sieve, and set aside.

2.3. Fourier transform infrared spectroscopy (FTIR)

A Fourier transform infrared spectrometer (VERTEX 70, Bruker, Germany) was used to determine the infrared spectra of the lyophilized samples with different retrogradation days. The method of determination was referred to the description by Xiao et al. (2021). The samples and KBr were ground in an onyx mortar with a ratio of 1:100 and subsequently scanned throughout the range of 400–4000 cm^{-1}. All spectra were deconvoluted by OMNIC 8.0 software (Nicolet, Inc., USA) to calculate the peak intensity ratio at 1047/1022 cm^{-1}.

2.4. X-ray diffraction (XRD)

XRD spectra of lyophilized samples with different days of retrogradation were determined using an X-ray diffractometer (D/MAX2500, Rigaku, Japan). The X-ray source used was Cu-Ka, and the samples were subjected to scanning at a rate of 5°/min, with a power of 40 kV, a current of 40 mA, and a step size of 0.02°. The MDI-Jade 6.0 program (Materials Data Ltd., USA) was used to compute the relative crystallinity of the X-ray diffractograms within the 5–40° range.

2.5. ^{13}C cross-polarization/magic angle spinning nuclear magnetic resonance (CP/MAS NMR) spectroscopy

The helical structure of lyophilized samples with different days of retrogradation was determined using a ^{13}C CP/MAS NMR (AVANCE NEO 400 WB, Bruker, Germany). The NMR test parameters were set at a speed of 6 kHz, a rotation angle of 54.7°, a crosspolarization contact time of 1 ms and a delay time of 3 s. At least 2400 times were scanned for each spectrum at room temperature to obtain a satisfactory signal-noise ratio. Amorphous, single-helix, and double-helix starch contents were computed using the procedure introduced by Tan et al. (2007).

2.6. Differential scanning calorimeter (DSC)

The retrogradation characteristics of the samples during storage at 4 °C were determined using DSC (Discovery SDT650, TA Instruments, New Castle, DE, USA). Samples taken after complete pasteurization and stored at 4 °C for 1, 7, 14 and 21 days were subjected to DSC measurements as described by Ge et al. (2021).

In order to accurately assess the rate of recrystallization and the type of nucleation of the samples during retrogradation, the enthalpy change of retrogradation of all the sample gels during storage was further analyzed using the following Avrami equation to resolve the retrogradation kinetic process of the samples.

$$X(t) = \frac{\Delta H_t - \Delta H_0}{\Delta H_\infty - \Delta H_0} = 1 - exp(-kt^n)$$

$$ln\left(-ln\left(1 - \frac{\Delta H_\infty}{\Delta H_\infty - \Delta H_t}\right)\right) = lnk + nlnt$$

where ΔH_0 was the enthalpy of retrogradation of the sample stored for 0 days (J/g); ΔH_t was the enthalpy of retrogradation of the sample stored for t days (J/g); ΔH_∞ was the maximum enthalpy of retrogradation of

the sample measured (J/g); t was the number of days of storage (d); k was the rate constant of starch retrogradation; and n was the Avrami index.

2.7. Determination of dynamic viscoelastic

The way in which starch molecule chains came together during retrogradation might also be seen in the alteration of the rheological modulus. Sample gels with different retrogradation days were removed and placed on a rheometer (MCR302, Anton Paar GmbH, Austria) with a 25 mm flat plate and a gap of 1 mm between the plate and the stage. The strain conditions were specified as $\gamma = 1$ %, and the frequency range was defined as 0.1–100 rad/s to get the curves depicting the changes in the energy storage modulus (G′) and loss modulus (G″) with respect to shear frequency.

2.8. Determination of gel firmness

The textural properties of gels in samples with different retrogradation times were determined using the TA-XT Plus Texture Meter Instrument (Stable Micro Systems Co. Ltd., Godalming, Surrey, UK). The gel underwent compression to 40 % of its original thickness using a cylindrical probe (P/0.5) in the TPA measuring mode of the physical analyzer. The test conditions were defined as follows: the pre-test, test, and post-test speeds were set at 1.5, 1, and 1 mm/s, respectively. The trigger type was automated with a force of 3 g, and the highest force measured represented the hardness of the gel.

2.9. Determination of low field strength nuclear magnetic resonance (LF-NMR)

The water mobility of the samples was assessed during storage for different time periods using an LF-NMR analyzer (Meso MR23-040 *V*-I, Niumag Electric Co., Shanghai, China) that operated at a proton resonance frequency of 20 MHz. Prior to measurement, all samples reached thermal equilibrium at a temperature of 25 °C for a duration of 30 min. The gels obtained from the samples at different stages of retrogradation were placed in glass NMR tubes of 40 mm in diameter. The transverse relaxation time (T_2) was calculated using a Carr-Purcell-Meiboom-Gill (CPMG) sequence. This sequence involved applying 90° and 180° pulses with durations of 10.40 and 21.20 μs, respectively. The waiting time (TW) between pulses was set to 4000 ms. The number of echoes (NECH) was 12,500, and the time to echo (TE) was 0.16 ms. The experiment was repeated 8 times (NS = 8), and the inversion spectrum of T_2 was obtained using MultiExp Inv Analysis software.

2.10. Statistics and analysis of data

SPSS 21.0 software (IBM, USA) was used to process the experimental data. The Duncan significance test was used to ascertain significant disparities in all statistical studies, and the program Origin 2022 (Origin Lab, Inc., USA) was utilized for the purpose of graphing.

3. Results and discussion

3.1. Analysis of short-range ordered structures

Fig. 1A displays the FTIR spectra of all the samples throughout the retrogradation period of 1 and 21 days. No further absorption peaks emerged or vanished throughout the retrogradation of the samples, suggesting that no novel functional groups were generated and no fresh covalent connections were established over the 21-day retrogradation period. The samples exhibited a characteristic C—H stretching vibration peak at 2930 cm^{-1} and a well defined wide peak at 3600–3000 cm^{-1}, indicating the presence of an O—H stretching vibration peak (Yang, Tang, et al., 2021).

The short-range ordered structure of starch might be defined by the fingerprint feature band at 1200–800 cm^{-1}, and the deconvolution spectra are displayed in Fig. 1B. The peak observed at a wavenumber of 1047 cm^{-1} was associated with the crystalline regions of starch, while the absorbance at 1022 cm^{-1} indicated the presence of amorphous areas. Thus, the short-range ordered structure of starch was characterized by the ratio of absorbance at the two specific locations. Usually, the degree of starch retrogradation increased as the $R_{1047/1022}$ ratio became bigger (Osevenou and J. R. M, 2002). The 1047/1022 cm^{-1} absorbance ratios of all samples are shown in Table 1. Proteins significantly affected the short-range ordered structure during starch retrogradation before and after postharvest ripening. The degree of short-range order increased by 0.252 % (JD-0) and 0.481 % (JD-40) for the samples with protein removed at 1 day of storage, respectively. The decline of short-range order of starch molecules was linked to the interactions between the starch molecules and the protein functional groups (Zhang et al., 2019). The presence of postharvest ripening reduced the extent to which proteins inhibited the short-range order in short-term starch retrogradation. This was because the interactions between starch and proteins weaken after postharvest ripening.

After 21 days of starch retrogradation, the short-range ordered structure in all samples increased significantly. The starch molecular chains underwent rearrangement during storage, which caused recrystallization and ultimately led to a rise in the short-range ordered structure. The absorbance ratios of JD-0 and JD-0-DP samples increased by 0.0086 and 0.0109 at 21 days of starch retrogradation, respectively, compared with 1 day of retrogradation. And the removal of protein samples significantly improved the short-range ordered structure of starch during long-term retrogradation. It indicated that the molecular chains of the protein removal samples were more likely to undergo rearrangement and produce more crystalline structures.

3.2. Crystalline structure analysis

XRD is commonly used to measure starch crystal properties and long-range ordered structures. Fig. 1D represents the XRD patterns of starch-protein complexes at 1 and 21 days of starch retrogradation and starch after protein removal. Usually, natural corn starch has significant peaks in the 2θ peaks at 15.3°, 17.3°, 18°, and 23°, which are typical of A-type starches. After pasting, the crystalline peaks of the starch partially disappeared, and all samples had a distinct peak at 17°, which presented a different XRD pattern from that of natural corn starch, demonstrating a characteristic B-type starch arrangement (Wu et al., 2023). Furthermore, a distinct peak at 2θ about 20° was seen in all samples, indicating a *V*-shaped XRD pattern. This was likely caused by the production of a complex consisting of amylose and lipids. By forming hydrogen bonds with the hydroxyl and water groups of the starch, the hydrophilic groups of the protein probably prevented hydrophobic interactions between the starch chains (Niu, Zhang, et al., 2018).

The relative crystallinity of all samples was determined using Jade software fitting, as shown in Table 1. The samples showed a significant increase in relative crystallinity during the 1–21 day period of starch retrogradation. This increase could be attributed to the binding of amylose and amylopectin molecules, and the formation of the double helix structure during long-term retrogradation (Soler et al., 2020).

As the duration of retrogradation increased from 1 to 21 days, the relative crystallinity of the complexes increased by 28.89 % (JD-0) and 20.81 % (JD-40), respectively. Similarly, the removal of proteins led to an increase in the relative crystallinity of the samples by 33.87 % (JD-0-DP) and 36.76 % (JD-40-DP), respectively. This was because the presence of proteins might impede the establishment of intermolecular hydrogen bonds in starch molecules during the process of retrogradation. In addition, corn proteins had a high content of zein, which had poor hydration characteristics and whose presence limited the contact between starch molecules and water molecules. Removal of the protein also led to an increase in the specific surface area of the starch granules,

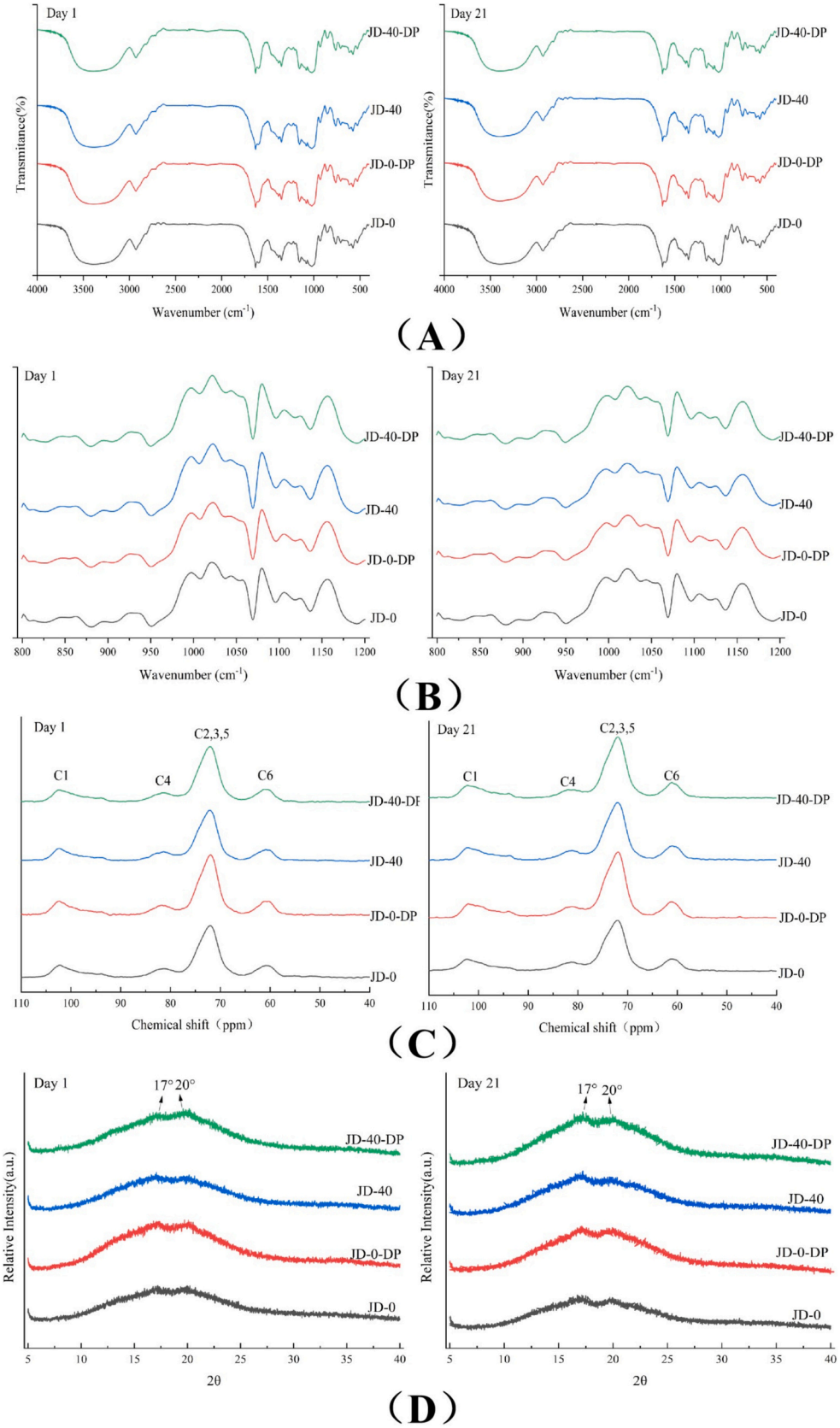

Fig. 1. (A) FTIR spectra; (B) deconvolution spectra of FTIR; (C) ^{13}C CP/MAS NMR spectra; (D) XRD plots of all samples during the storage period.

Table 1
Parameters of short-range order, relative crystallinity, and helical structure of samples during retrogradation.

Samples	Retrogradation days	1047/1022 cm^{-1}	Relative crystallinity (%)	Single helix content (%)	Double helix content (%)	Amorphous starch content(%)
JD-0	1d	0.7554 ± 0.0001^{f}	4.88 ± 0.34^{d}	1.87 ± 0.32^{d}	8.27 ± 1.43^{e}	89.86 ± 1.11^{a}
	21d	0.7640 ± 0.0002^{d}	6.29 ± 0.47^{b}	2.27 ± 0.17^{bc}	15.24 ± 2.60^{c}	82.49 ± 2.74^{c}
JD-0-DP	1d	0.7573 ± 0.0001^{e}	5.64 ± 0.27^{bc}	2.05 ± 0.14^{cd}	17.45 ± 0.51^{c}	80.50 ± 0.45^{c}
	21d	0.7682 ± 0.0007^{c}	7.55 ± 0.57^{a}	2.94 ± 0.15^{a}	25.25 ± 1.64^{a}	71.81 ± 1.65^{e}
JD-40	1d	0.7479 ± 0.0003^{h}	5.19 ± 0.43^{cd}	1.93 ± 0.17^{c}	6.28 ± 0.71^{e}	91.79 ± 0.87^{a}
	21d	0.7889 ± 0.0015^{a}	6.27 ± 0.17^{b}	2.54 ± 0.08^{b}	11.87 ± 0.72^{d}	85.59 ± 0.67^{b}
JD-40-DP	1d	0.7515 ± 0.0007^{g}	5.74 ± 0.36^{bc}	2.19 ± 0.21^{cd}	16.49 ± 0.73^{c}	81.32 ± 0.69^{c}
	21d	0.7760 ± 0.0012^{b}	7.85 ± 0.34^{a}	3.01 ± 0.07^{a}	20.58 ± 0.84^{b}	76.41 ± 0.78^{d}

Different letters in the same column indicate significant differences ($p < 0.05$).

and the open starch granule structure accelerated the penetration of water molecules. During the starch pasting process, starch rapidly absorbed water and swelled. Amylose was easily leached out during shearing. Amylose and amylopectin lost the restriction of protein interactions, increasing the mobility of starch chains, and hydrogen bonding between starch chains was more likely to be formed during starch retrogradation, which promoted recrystallization of starch molecules. This outcome also demonstrated that the interaction between starch and protein significantly inhibited the retrogradation of starch. Thus, it could be seen that proteins had a stronger inhibitory effect on the recrystallization of samples that had not been ripened during the retrogradation process.

3.3. Helix structure analysis

The ^{13}C CP/MAS NMR spectra and helical structures of all samples during retrogradation are shown in Fig. 1C and Table 1. The C1 and C4 peaks seen in the NMR spectrograms were closely linked to the helical and amorphous structures of starch retrogradation, respectively (Gidley & Bociek, 1985). After 1–21 days of retrogradation for all samples, the ratios of single helix and double helix increased significantly, whereas the proportion of amorphous content decreased significantly. The conclusions agreed with the outcomes of prior investigations about the ratio of 1047/1022 cm^{-1} and the relative crystallinity. This was caused by the recrystallization that occurred during retrogradation and the increase in ordered structures. Starch retrogradation was split into short-term retrogradation stage and long-term retrogradation stage. Immediately after starch pasting, there was a temporary process called short-term retrogradation. This process mostly included the amylose molecules connecting to each other by hydrogen bonding, resulting in the formation of a three-dimensional gelatinous mesh structure. The nuclei generated by amylose during the first step of starch retrogradation provided a crystalline seed source for long-term aging, allowing the amylopectin crystalline zone to grow and form crystals centered on this nucleus (Liu et al., 2024).

At 1 day of retrogradation, the double helix content of the samples was 8.27 % (JD-0), 17.45 % (JD-0-DP), 6.28 % (JD-40) and 16.49 % (JD-40-DP). The double helix concentration of the samples at 21 days of retrogradation increased by 84.28 % (JD-0), 44.70 % (JD-0-DP), 89.01 % (JD-40), and 24.80 % (JD-40-DP), respectively, compared to 1 day of retrogradation. Proteins primarily hindered the formation of hydrogen bonds between amylose, which was essential for the development of crystalline nuclei, through hydrophobic interactions. This interaction affected the formation of the double helix during starch retrogradation (Hu et al., 2020; Kuang et al., 2022; Niu, Han, et al., 2018), ultimately resulting in the inhibition of the entire aging process. On the other hand, hydrogen bonding (Xiao & Zhong, 2017; Yang et al., 2019) and electrostatic interactions (Lu et al., 2016) between proteins and amylopectin retarded double helix generation during starch retrogradation. Chen et al. (2021) showed that positively charged lysine inhibited the retrogradation of corn starch. Nevertheless, the direct electrostatic contacts between starch and protein were feeble as a result of the low phosphate level present in corn starch. More probably, strongly soluble amino acids, including aspartic acid and lysine, formed hydrogen bonds with the starch to prevent it from recrystallizing.

After protein removal, the double helix content of the samples after 1 day of retrogradation increased by 1.11 times (JD-0) and 1.63 times (JD-40), respectively. The double helix concentration of the samples after 21 days of retrogradation increased by 65.68 % (JD-0) and 73.38 % (JD-40), respectively, which was consistent with the previous XRD analysis. The findings demonstrated that the proteins had a greater effect on preventing the retrogradation of starch before postharvest ripening compared to after postharvest ripening. This was because the hydrophobic interactions and hydrogen bonding between starch and proteins were weakened in the postharvest ripened samples.

3.4. Enthalpy of retrogradation and retrogradation kinetic analysis

The enthalpy of retrogradation of the samples during storage is shown in Table 2. The enthalpy of retrogradation for all the samples exhibited a substantial rise as the retrogradation period increased. The enthalpy of retrogradation increased to 3.206 J/g (JD-0), 4.93 J/g (JD-0-DP), 3.503 J/g (JD-40), and 4.876 J/g (JD-40-DP) for all samples at retrogradation times of 1–21 days, respectively. The observed phenomena might be explained by the reorganization of the molecular chains of starch retrogradation that occurred during storage. This finding was in line with the XRD data.

At 1 day of retrogradation, the enthalpy of the sample JD-0-DP after protein removal increased to 1.2839 J/g, which was 1.014 times higher. The enthalpy of JD-40-DP was increased by 51.98 % compared to the complex. The presence of the protein inhibited the ability of amylose to form nuclei through hydrogen bonding during short-term retrogradation, reducing the rate of recrystallization. At 7 days of retrogradation, the enthalpy of the samples increased by 1.10 times (JD-0) and 95.43 % (JD-40) after the removal of protein. At 14 days of retrogradation, the enthalpy of the samples increased by 90.80 % (JD-0) and 82.01 % (JD-40) after the removal of protein. At 21 days of retrogradation, the enthalpy of the samples increased by 53.74 % (JD-0) and 39.19 % (JD-40) after the removal of protein. The protein prevented the long-term retrogradation of amylopectin, which was the process of intermolecular hydrogen bond formation between amylopectin molecules and the recrystallization of starch molecules. The enthalpy of heat absorption of starch increased more significantly in samples without postharvest ripening compared to samples that underwent postharvest ripening. This was because postharvest ripening reduced the interactions between starch and protein, leading to a narrower tendency for amylopectin to change between complexes as well as between samples with proteins removed (Hu et al., 2024).

The crystallographic data were modeled using the Avrami equation by fitting the experimental data of retrogradation enthalpy to the nonlinear regression equation. The results are shown in Fig. 2A-D. The starch retrogradation kinetic parameters were acquired by evaluating the retrogradation kinetic curves of the samples before and after postharvest ripening, and the findings were reported in Table 2. Previous research had acknowledged the Avrami equation as a useful method for analyzing the kinetics of starch recrystallization (Niu et al., 2017).

Table 2
Enthalpy of retrogradation and kinetic parameters of retrogradation of the sample during retrogradation process.

Samples	Retrogradation enthalpy ΔH(J/g)				Avrami equation	n	lnk	k	R^2
	1d	7d	14d	21d					
JD-0	−0.6374 ± 0.0715[a]	−1.8310 ± 0.1115[c]	−2.4890 ± 0.2126[d]	−3.2060 ± 0.1785[e]	y = 0.71628×-1.51778	0.7163 ± 0.0280	−1.5178 ± 0.0529	0.21920	0.99696
JD-0-DP	−1.2839 ± 0.3206[b]	−3.8370 ± 0.4206[f]	−4.7490 ± 0.2886[g]	−4.9300 ± 0.3746[g]	y = 0.88953× − 1.22394	0.8895 ± 0.0639	-1.2239 ± 0.1209	0.29407	0.98975
JD-40	−0.7389 ± 0.2149[a]	−1.9260 ± 0.3749[c]	−2.6097 ± 0.4626[d]	−3.5030 ± 0.5226[ef]	y = 0.65535× − 1.45272	0.6554 ± 0.0315	-1.4527 ± 0.0597	0.23393	0.99538
JD-40-DP	−1.1230 ± 0.1226[ab]	−3.7640 ± 0.2785[f]	−4.7500 ± 0.3165[g]	−4.8760 ± 0.1775[g]	y = 0.97531×-1.37498	0.9753 ± 0.0867	−1.3750 ± 0.1641	0.25284	0.98432

Different letters in the table indicate significant differences ($p < 0.05$).

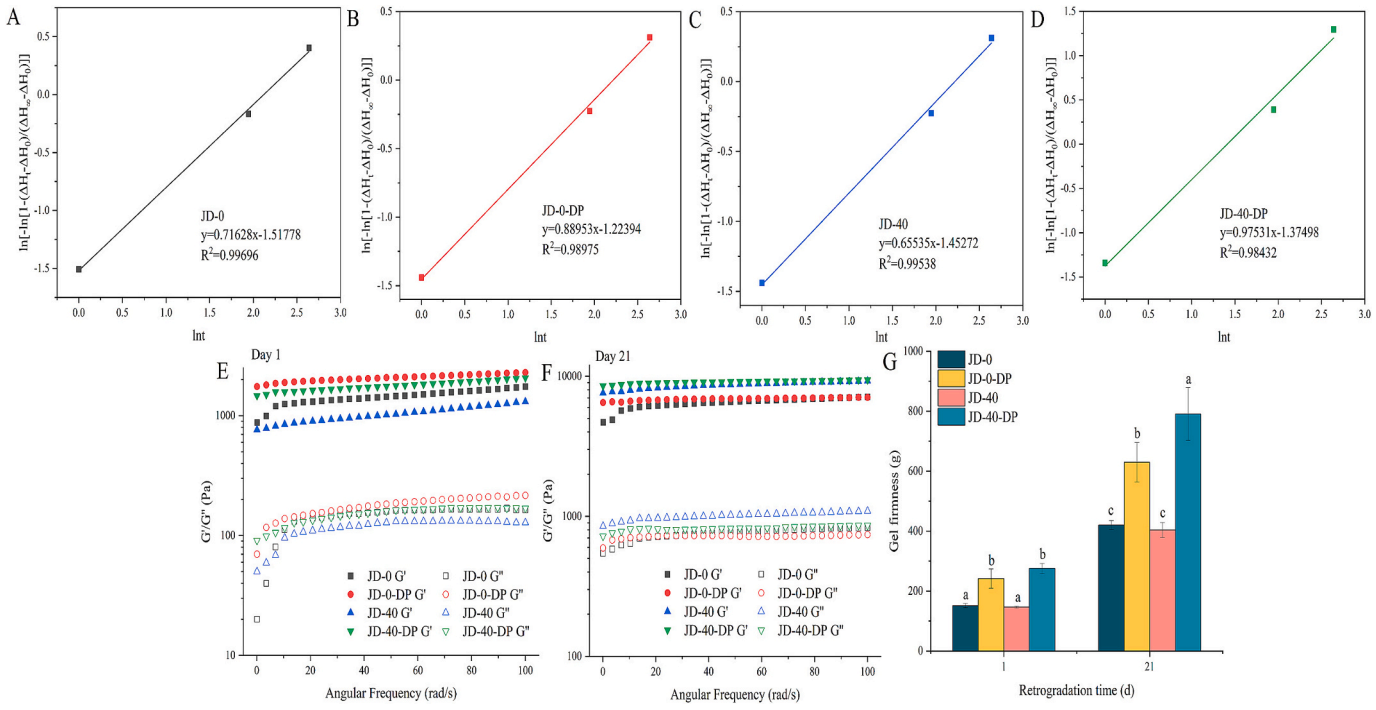

Fig. 2. Sample retrogradation kinetic curves (A. JD-0; B. JD-0-DP; C. JD-40; D. JD-40-DP), dynamic rheological properties of the samples during retrogradation (E. 1d; F. 21d), and (G) gel firmness.

The Avrami parameters are shown in Table 2. The R^2 values of all the samples were higher than 0.98, suggesting a relatively good fitting outcome. The Avrami index n measured the crystal nucleation and growth process. All the samples had an index n less than 1, which was consistent with the results of Niu et al. (2017). This indicated that all of their nucleation mechanisms were primary nucleation (Chen et al., 2021). The parameter k denoted the rate constant for crystal development, with larger values of k indicating a faster rate of starch crystallization. The findings revealed that the value of k of the samples containing protein were lower than that of the samples from which protein had been removed. This demonstrated that the presence of protein slowed down the rate of recrystallization of starch molecules. After protein removal, the k values of the samples exhibited a 34.16 % rise before postharvest ripening (JD-0) and an 8.1 % increase after postharvest ripening (JD-40), suggesting that protein inhibited starch retrogradation more significantly before postharvest ripening. In conclusion, the presence of proteins slowed down the rate of starch retrogradation, and corn proteins might be a potential anti-retrogradation additive to extend the duration of freshness for food products made from corn starch.

3.5. Dynamic viscoelastic analysis

The dynamic rheological profiles of the samples during retrogradation are presented in Fig. 2E-F. During the cooling and early gelatinization of starch, the swelling of starch granules and the three-dimensional network structure formed by amylose produced the elasticity and strength of the gel, so G' usually reflected the degree of retrogradation of amylose. Fig. 2E showed the viscoelasticity of the starch gels when the samples were stored for 1 day, and the G′ of all the samples were ordered from largest to smallest as JD-0-DP, JD-40-DP, JD-0, and JD-40, and the results were consistent with those of the short-range ordered structures. The higher elasticity of the samples with proteins removed compared to the complexes was hypothesized to be the result of a combination of two mechanisms. The first possible mechanism was that proteins obstructed the process of starch gelation by reducing the surface area of starch molecules in contact with water, increasing the spacing between starch chains, and impeding the formation of hydrogen bonds between starch molecules. The second possible mechanism was the interference of proteins with the movement of starch molecular chains in the system via hydrophobic interactions. This interference brought about a decrease in the mobility of the starch chains and hindered the recrystallization process (Chen et al., 2019). In

addition, Wu et al. (2023) examined the impact of rice proteins on the pasting and starch retrogradation characteristics of rice starch and discovered that the presence of proteins could reduce the degree of damage to starch gels, forming a more compact network structure, increasing the thickness of the pore wall of the starch network structure, and making the pore size of the starch network structure smaller and more uniform. In contrast, in the composite system of corn starch and protein, there was a lack of compatibility between the two components. Protein restrained the rearrangement of starch molecules, and enhanced the water retention ability of the starch gel, and facilitated the development of the network structure. Corn zein reduced the density and homogeneity of the gel, and inhibited the aggregation of protein and starch macromolecules through intermolecular interactions, weakening the gel network and resulting in a decrease in the elasticity of the starch gel. Kuang et al. (2022) also discovered that the addition of reconstituted gluten fractions inhibited the formation of elastic components in the three-dimensional networked starch gel structure of wheat starch by suppressing amylose gelatinization, which was a key factor in delaying short-term retrogradation. The loss modulus (G″) of the sample retrogradation for 1 day in Fig. 2E represented the rheological analysis that represented the transient molecular network structure of the pasted starch and its viscous characteristics. Corn proteins decreased the viscosity of starch gels undergoing short-term retrogradation.

Fig. 2F showed the gel viscoelasticity of all samples stored for 21 days. Compared with Fig. 2E, both G′ and G″ of the 21-day retrogradation samples exhibited a considerable rise, suggesting a continuous enhancement in gel strength and hardness throughout the retrogradation process. The elevated G′ and G″ values were a result of the reaggregation and entanglement of starch molecules (Zeng et al., 2022).

3.6. Gel firmness analysis

The increase in firmness of the pasted starch during storage was strongly associated with retrogradation and was commonly employed to assess the degree of retrogradation (Wang et al., 2015; Yang, Dhital, et al., 2021). Starch retrogradation could result in an increase in the hardness of starch-based foods. Fig. 2G showed the effect of protein on the gel firmness of the samples before and after post ripening retrogradation for 1 and 21 days. The gel firmness of all samples enhanced with time during storage. At 1 day of retrogradation, the gel firmness of starch and protein complexes JD-0 and JD-40 was 151.41 g and 146.37 g, respectively, which showed no significant variation between the samples but was significantly lower than the samples with protein removed, JD-0-DP and JD-40-DP. After protein removal, JD-0-DP and JD-40-DP increased to 241.60 g and 275.64 g, respectively. Starch gels with proteins removed had a stronger firmness during starch retrogradation, and starch molecules were more readily bonded to each other by hydrogen bonding, which contributed to the creation of a relatively ordered and stable crystalline structure and boosted the strength of the gel. Hu et al. (2020) also showed that the reduction in the stiffness of starch gels with the addition of whey isolate protein hydrolysate was caused by the interaction between starch molecules and protein hydrolysate products. This interaction hindered the formation of hydrogen bonds between starch chains, resulting in alterations to the overall structure of the starch gels at both the long-range and short-range levels. Moreover, through Fig. 2G, we found that after postharvest ripening, the gel strength of the protein-removed samples increased to different extents. This suggested that the ripening process facilitated the entanglement and interaction of starch molecular chains, thereby forming a stronger gel network structure, which was in line with our previous research results (Hu et al., 2023).

3.7. Moisture migration analysis

The use of LF-NMR proved to be a very efficient method for investigating the movement of water inside starch systems. In addition to the recrystallization of starch molecules, the retrogradation process also involved the dehydration contraction of gels, which was mainly reflected in the fluidity of water. The spin relaxation time (T_2) obtained from LF-NMR analysis could reply the difference in the degree of freedom of water molecules. The impact of protein on water migration during retrogradation of samples before and after postharvest ripening was shown in Fig. 3A-B. Generally, pasted starch demonstrated four CPMG proton clusters: T_{2b} (0.05–5 ms), T_{21} (5–45 ms), T_{22} (50–300 ms), and T_{23} (1000–4000 ms), which represented strongly bound water, semi-bound water, weakly bound water, and free water, respectively. All samples showed a gradual decrease in the peak value of weakly bound water and an increase in the peak value of free water as the retrogradation time increased. This was due to the starch molecules reorganizing during retrogradation, which weakened their ability to bind water molecules and caused the starch gel to lose water and contract, leading to an increase in free water over time.

To gain more insight into water mobility during gel retrogradation, relaxation times (T_{2b}, T_{21}, T_{22}, and T_{23}) and peak area ratios (A_{2b}, A_{21}, A_{22}, and A_{23}) were calculated from NMR data obtained from multiple exponential fits. As can be seen from Fig. 3A-C, following starch retrogradation, the peaks associated with semi-bound water and highly bound water shifted towards shorter relaxation durations, suggesting that the fluidity of water decreased, and the system became more restrictive towards water molecules. This effect tended to align with the process that led to the formation of intertwined double helix structures in starch molecules, thus restricting the mobility of water. The increase in the peak area of free water in the sample with a long retrogradation time compared to the sample with a short retrogradation time might be due to the loosening of the starch network after retrogradation, which attenuated the number of water molecules bound. In addition, the presence of proteins restricted the intermolecular cross-linking of starch, thereby limiting the creation of ordered structures, a conclusion that was consistent with the trend of ordered structure studies. Proteins caused a reduction in the strength of the bonds between water and the starch network, thereby increasing water mobility. The pasting treatment could unfold the proteins, thereby exposing hydrophobic residues (Li et al., 2020), which might potentially cause water to be repelled by the starch granules, restricting their swelling and molecular movement. Kuang et al. (2022) discovered that hydrophobic gluten polypeptides could limit retrogradation of amylopectin by this mechanism. Therefore, proteins might enhance the ability of gels to retain water by preventing retrogradation. After the removal of protein, the increase in the proportion of free water A_{23} in the sample without postharvest ripening was higher than that in the post-ripened sample. This indicated that proteins played a larger role in enhancing the water-holding ability of the starch gels in the sample that did not undergo postharvest ripening during retrogradation process.

3.8. Mechanisms of endogenous protein effects on starch retrogradation characteristics of corn before and after postharvest ripening

Fig. 4 revealed the mechanism by which endogenous proteins affect the starch retrogradation characteristics of corn before and after postharvest ripening. The presence of proteins in corn, whether or not it had been post-harvest ripened, prevented the enlargement and bursting of starch granules during the process of pasting, thus slowing down the process of starch pasting and starch retrogradation. This was, on one hand, due to the fact that corn proteins existed between starch granules, which created a spatial site-blocking effect on the forming of starch gel, reducing the area of starch molecules in contact with water molecules and increasing the spacing between starch polymer strands, thus slowing down the recrystallization of starch. On the other hand, our previous studies had confirmed that there were mainly hydrophobic interactions and hydrogen bonding between starch and proteins (Hu et al., 2024). The complex samples underwent gelatinization, and the zein unfolded, exposing hydrophobic residues such as alanine, leucine, proline, and

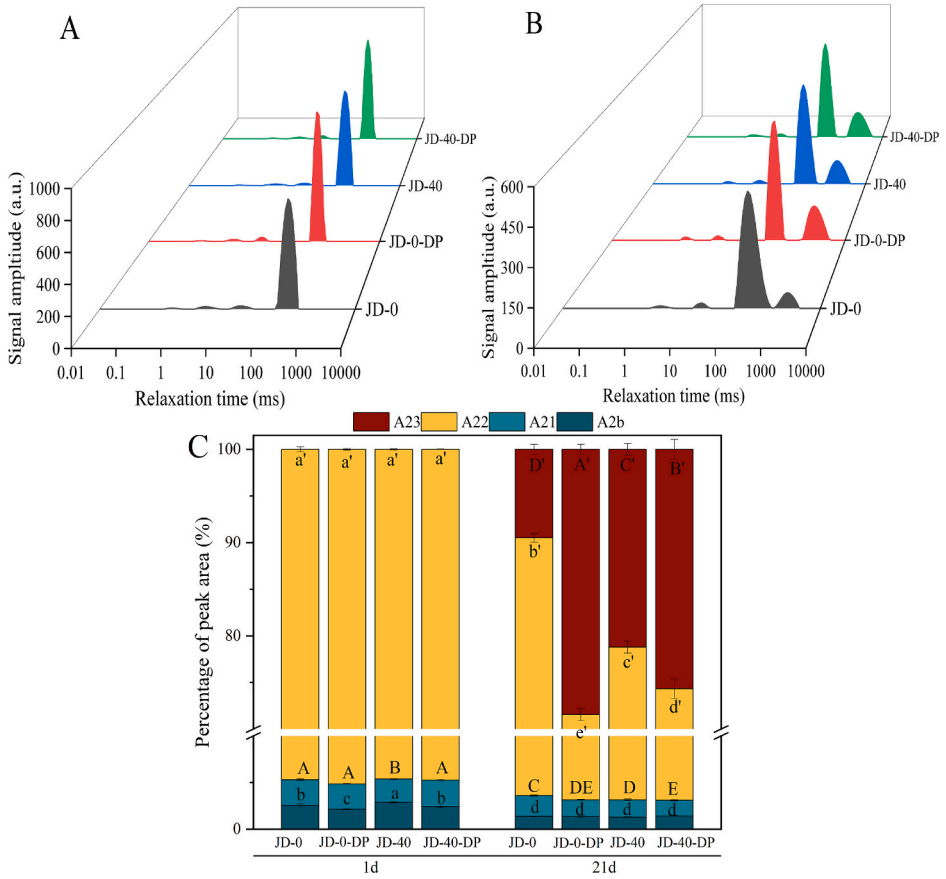

Fig. 3. Moisture migration of samples during retrogradation (A. 1d; B. 21d) and (C) percent relaxation area.

phenylalanine. These hydrophobic amino acids would repel the water in the starch granules, restricting swelling and molecular migration, thereby inhibiting the retrogradation of starch. Secondly, the presence of hydrogen bonding between starch and protein effectively hindered the process of starch retrogradation. Consequently, the existence of proteins reduced the relative crystallinity and double helix formation during retrogradation (Table 1), impeded intermolecular hydrogen bonding of starch, and inhibited recrystallization of starch chains, leading to a weakening of the viscoelasticity and firmness of the starch gels (Fig. 2E-G). After the sample underwent retrogradation, starch molecules formed intercross-linked double helix structures, reducing the mobility of water. However, the presence of protein weakened the transformation of bound water into free water, enhanced the water-holding capacity, and inhibited the shrinkage of starch gel during storage (Fig. 3).

Postharvest ripening brought about a decrease in the interaction between starch and protein (Hu et al., 2024). Therefore, in the samples that had undergone postharvest ripening, the inhibitory effect of proteins on the increase in short-range order, relative crystallinity, and double helix structure of starch during retrogradation was lower than that in the samples that had not undergone postharvest ripening.

4. Conclusions

This work investigated the impact of endogenous proteins in corn on the retrogradation characteristics of starch before and after postharvest ripening, and explored the underlying mechanisms. Protein-starch interactions could hinder the formation of intermolecular hydrogen bonds in starch molecules during retrogradation and inhibit the formation of short-range order, relative crystallinity, and double-helical structures during recrystallisation. The aggregation of protein and starch macromolecules was inhibited through intermolecular interactions, weakening the gel network, which led to a decrease in gel viscoelasticity and firmness. Furthermore, proteins could inhibit starch retrogradation by preventing cross-linking between starch molecules, restricting the migration of water molecules, enhancing the water-holding capacity of starch gels. In summary, corn protein could be used as an anti-starch retrogradation additive to extend the shelf life of corn starch-based foods. In particular, the role of corn proteins was more significant in corn that was not ripened post-harvest. Further studies should focus on the effect of the structure and properties of endogenous proteins in corn on starch retrogradation and their stability under various processing conditions. The results of this study provided strong evidence for the effect of protein on starch retrogradation in corn-based food processing before and after postharvest ripening. It contributed to the development of healthy and nutritious starch products by elucidating the underlying mechanisms of this process.

CRediT authorship contribution statement

Nannan Hu: Writing – original draft, Methodology. **Weihua Qi:** Writing – review & editing, Data curation, Conceptualization. **Jinying Zhu:** Software, Resources. **Fuyin Zhao:** Investigation, Formal analysis. **Lin Xiu:** Writing – review & editing, Visualization. **Mingzhu Zheng:** Writing – review & editing, Supervision, Project administration. **Jingsheng Liu:** Validation, Funding acquisition.

Declaration of competing interest

The authors declared that they have no conflicts of interest to this work. We declare that we do not have any commercial or associative interest that represents a conflict of interest in connection with the work

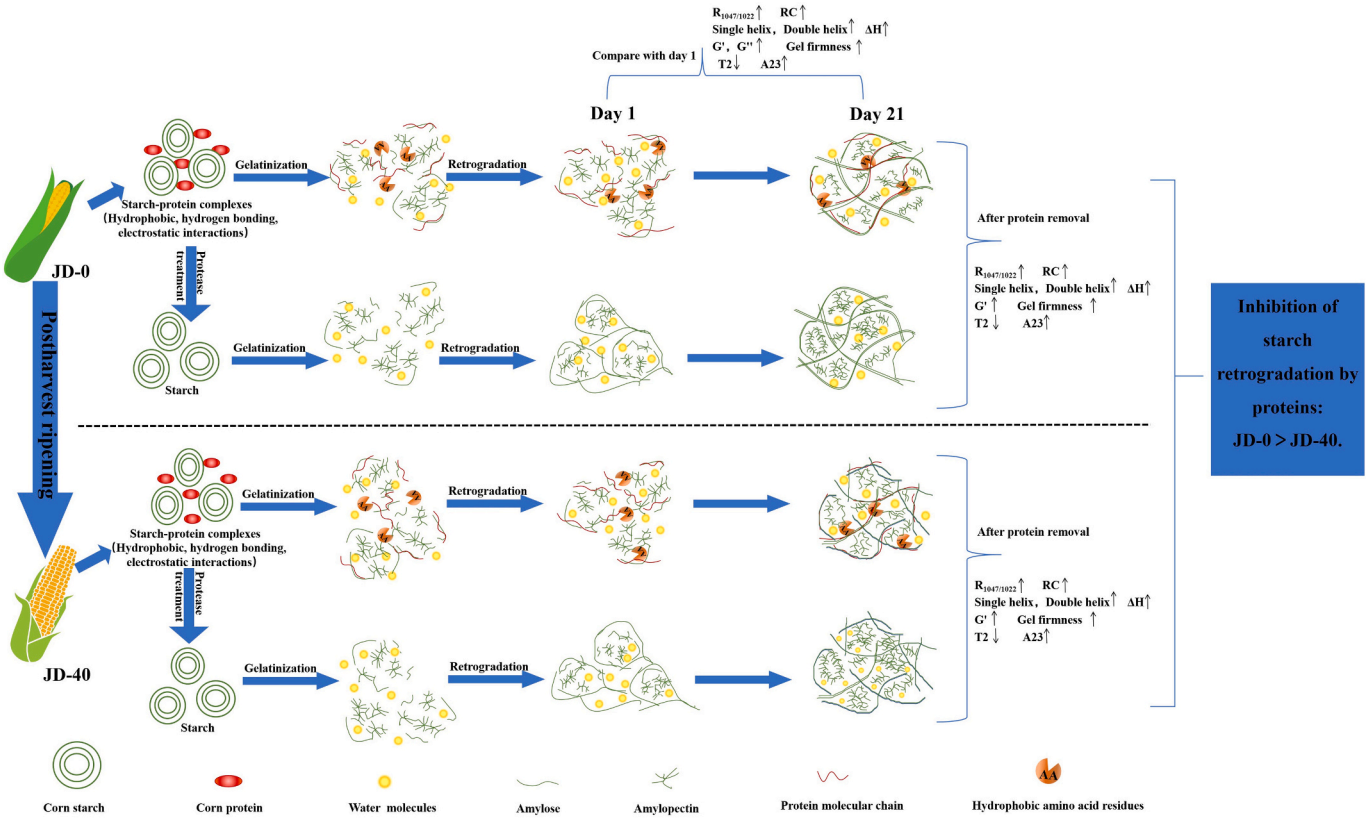

Fig. 4. Mechanism of starch-protein interactions on starch retrogradation characteristics during corn postharvest ripening process.

submitted.

Acknowledgments

This work was supported by the Joint Funds of the National Natural Science Foundation of China (No. U23A20257), and the Science and Technology Development Program of Jilin Province of China (No. 20210202108NC).

Data availability

The authors do not have permission to share data.

References

Chen, B., Wang, Y.-R., Fan, J.-L., Yang, Q., & Chen, H.-Q. (2019). Effect of glutenin and gliadin modified by protein-glutaminase on retrogradation properties and digestibility of potato starch. *Food Chemistry, 301*, Article 125226.

Chen, Y., Wang, Y.-S., Zhang, X., & Chen, H.-H. (2021). Retardant effect of different charge-carrying amino acids on the long-term retrogradation of normal corn starch gel. *International Journal of Biological Macromolecules, 189*, 1020–1028.

Ge, X., Shen, H., Su, C., Zhang, B., Zhang, Q., Jiang, H., et al. (2021). The improving effects of cold plasma on multi-scale structure, physicochemical and digestive properties of dry heated red adzuki bean starch. *Food Chemistry, 349*, Article 129159.

Gidley, M. J., & Bociek, S. M. (1985). Molecular organization in starches: A carbon 13 CP/MAS NMR study. *Journal of the American Chemical Society, 107*(24), 7040–7044.

Hu, N., Qi, W., Zhu, J., Li, S., Zheng, M., Zhao, C., & Liu, J. (2024). Postharvest ripening of newly harvested corn: Weakened interactions between starch and protein. *Food Chemistry, 451*, Article 139450.

Hu, N., Zhao, C., Li, S., Qi, W., Zhu, J., Zheng, M., & Liu, J. (2023). Postharvest ripening of newly harvested corn: Structural, rheological, and digestive characteristics of starch. *LWT- Food Science and Technology, 180*, Article 114728.

Hu, Y., He, C., Zhang, M., Zhang, L., Xiong, H., & Zhao, Q. (2020). Inhibition from whey protein hydrolysate on the retrogradation of gelatinized rice starch. *Food Hydrocolloids, 108*, Article 105840.

Kuang, J., Huang, J., Ma, W., Min, C., Pu, H., & Xiong, Y. L. (2022). Influence of reconstituted gluten fractions on the short-term and long-term retrogradation of wheat starch. *Food Hydrocolloids, 130*, Article 107716.

Li, B., Zhang, Y., Xu, F., Khan, M. R., Zhang, Y., Huang, C., & Liu, A. (2021). Supramolecular structure of *Artocarpus heterophyllus* lam seed starch prepared by improved extrusion cooking technology and its relationship with in vitro digestibility. *Food Chemistry, 336*, Article 127716.

Li, L., Yuan, T. Z., & Ai, Y. (2020). Development, structure and in vitro digestibility of type 3 resistant starch from acid-thinned and debranched pea and normal maize starches. *Food Chemistry, 318*, Article 126485.

Li, W., Gu, Z., Cheng, L., Li, Z., Li, C., Ban, X., & Hong, Y. (2023). Effect of endogenous proteins and heat treatment on the in vitro digestibility and physicochemical properties of corn flour. *Food Hydrocolloids, 135*, Article 108220.

Lian, X., Guo, J., Wang, D., Li, L., & Zhu, J. (2014). Effects of protein in wheat flour on Retrogradation of wheat starch. *Journal of Food Science, 79*(7–8–9), 1505–1511.

Lian, X., Zhu, W., Wen, Y., Li, L., & Zhao, X. (2013). Effects of soy protein hydrolysates on maize starch retrogradation studied by IR spectra and ESI-MS analysis. *International Journal of Biological Macromolecules, 59*, 143–150.

Liu, C., Liu, S., Li, R., Zhang, X., & Chang, X. (2024). A mechanistic study of chestnut starch retrogradation and its effects on in vitro starch digestion. *International Journal of Biological Macromolecules, 276*, Article 133803.

Lu, Z.-H., Donner, E., Yada, R. Y., & Liu, Q. (2016). Physicochemical properties and in vitro starch digestibility of potato starch/protein blends. *Carbohydrate Polymers, 154*, 214–222.

Nicolai, T., & Durand, D. (2013). Controlled food protein aggregation for new functionality. *Current Opinion in Colloid & Interface Science, 18*(4), 249–256.

Niu, H., Han, Q., Cao, C., Liu, Q., & Kong, B. (2018). Short-term retrogradation behaviour of corn starch is inhibited by the addition of porcine plasma protein hydrolysates. *International Journal of Biological Macromolecules, 115*, 393–400.

Niu, H., Zhang, M., Xia, X., Liu, Q., & Kong, B. (2018). Effect of porcine plasma protein hydrolysates on long-term retrogradation of corn starch. *Food Chemistry, 239*, 172–179.

Niu, L., Wu, L., & Xiao, J. (2017). Inhibition of gelatinized rice starch retrogradation by rice bran protein hydrolysates. *Carbohydrate Polymers, 175*, 311–319.

Osevenou, S. E. H., Farhat, I. A., & J. R. M. (2002). Organisation of the external region of the starch granule as determined by infrared spectroscopy. *International Journal of Biological Macromolecules, 31*, 79–85.

Scott, G., & Awika, J. M. (2023). Effect of protein-starch interactions on starch retrogradation and implications for food product quality. *Comprehensive Reviews in Food Science and Food Safety, 22*(3), 2081–2111.

Soler, A., Velazquez, G., Velazquez-Castillo, R., Morales-Sanchez, E., Osorio-Diaz, P., & Mendez-Montealvo, G. (2020). Retrogradation of autoclaved corn starches: Effect of water content on the resistant starch formation and structure. *Carbohydrate Research, 497*, Article 108137.

Tan, I., Flanagan, B. M., Halley, P. J., And, A., & Gidley, M. J. (2007). A method for estimating the nature and relative proportions of amorphous, single, and double

helical components in starch granules by (13)C CP/MAS NMR. *Biomacromolecules, 8* (3), 885–891.
Wang, S., Li, C., Copeland, L., Niu, Q., & Wang, S. (2015). Starch Retrogradation: A comprehensive review. *Comprehensive Reviews in Food Science and Food Safety, 14*(5), 568–585.
Wu, C., Gong, X., Zhang, J., Zhang, C., Qian, J.-Y., & Zhu, W. (2023). Effect of rice protein on the gelatinization and retrogradation properties of rice starch. *International Journal of Biological Macromolecules, 242*, Article 125061.
Xiao, J., & Zhong, Q. (2017). Suppression of retrogradation of gelatinized rice starch by anti-listerial grass carp protein hydrolysate. *Food Hydrocolloids, 72*, 338–345.
Xiao, Y., Wu, X., Zhang, B., Luo, F., Lin, Q., & Ding, Y. (2021). Understanding the aggregation structure, digestive and rheological properties of corn, potato, and pea starches modified by ultrasonic frequency. *International Journal of Biological Macromolecules, 189*, 1008–1019.
Yang, C., Zhong, F., Douglas Goff, H., & Li, Y. (2019). Study on starch-protein interactions and their effects on physicochemical and digestible properties of the blends. *Food Chemistry, 280*, 51–58.
Yang, H., Tang, M., Wu, W., Ding, W., Ding, B., & Wang, X. (2021). Study on inhibition effects and mechanism of wheat starch retrogradation by polyols. *Food Hydrocolloids, 121*, Article 106996.
Yang, S., Dhital, S., Shan, C.-S., Zhang, M.-N., & Chen, Z.-G. (2021). Ordered structural changes of retrograded starch gel over long-term storage in wet starch noodles. *Carbohydrate Polymers, 270*, Article 118367.
Zeng, X., Zheng, B., Xiao, G., & Chen, L. (2022). Synergistic effect of extrusion and polyphenol molecular interaction on the short/long-term retrogradation properties of chestnut starch. *Carbohydrate Polymers, 276*, Article 118731.
Zhang, M., Sun, C., Wang, X., Wang, N., & Zhou, Y. (2020). Effect of rice protein hydrolysates on the short-term and long-term retrogradation of wheat starch. *International Journal of Biological Macromolecules, 155*, 1169–1175.
Zhang, Y., Chen, C., Chen, Y., & Chen, Y. (2019). Effect of rice protein on the water mobility, water migration and microstructure of rice starch during retrogradation. *Food Hydrocolloids, 91*, 136–142.
Zhang, Y., Liu, W., Liu, C., Luo, S., Li, T., Liu, Y., & Zuo, Y. (2014). Retrogradation behaviour of high-amylose rice starch prepared by improved extrusion cooking technology. *Food Chemistry, 158*, 255–261.
Zhang, Y., Xu, F., Wang, Q., Zhang, Y., Wu, G., Tan, L., & Zhang, Z. (2022). Effects of moisture content on digestible fragments and molecular structures of high amylose jackfruit starch prepared by improved extrusion cooking technology. *Food Hydrocolloids, 133*, Article 108023.
Zhang, Y., Zuo, H., Xu, F., Zhu, K., Tan, L., Dong,W., Wu, G. (2021). The digestion mechanism of jackfruit seed starch using improved extrusion cooking technology. Food Hydrocolloids, 110, 106154.
Zhao, C., Li, Q., Hu, N., Yin, H., Wang, T., Dai, X., & Liu, J. (2022). Improvement of structural characteristics and in vitro digestion properties of zein by controlling postharvest ripening process of corn. *Food Control, 142*, Article 109221.